

# FACTORS INFLUENCING THE HEAT TRANSFER FROM CYLINDRICAL ANEMOMETER PROBES

M. R. DAVIS

School of Mechanical and Industrial Engineering, The University of New South Wales,  
P.O. Box 1, Kensington, N.S.W., 2033, Australia

and

P. O. A. L. DAVIES

Institute of Sound and Vibration Research, The University of Southampton, Southampton, SO9 5NH, England

(Received 9 February 1971 and in revised form 19 October 1971)

**Abstract**—It is often assumed that the calibrations of heated wire and film anemometer probes depend upon some relationship between the probe Nusselt number and Reynolds number based upon the component of flow velocity normal to the probe. In practice departures from such a simplified behaviour are met due to the influence of probe temperature, variations in molecular mean free path of the fluid, the conditions of finite heat transfer as zero flow speed is approached and the onset of three-dimensional effects in the cooling of yawed probes. In this paper the interacting effects of overhear ratio, Knudsen number, Péclet number, length to diameter ratio, Grashof number and yaw angle are discussed. In particular, results are presented which demonstrate the influence of the Péclet number and yaw angle upon the cooling relationships, the variation of non-linear heat transfer with Knudsen number and departures from symmetric responses in yawed flows. The measurements reported have been confined to cylindrical hot wire and hot film probes operated at constant resistance.

## NOMENCLATURE

$a$ ,	coefficient representing asymmetric heating of flow, equation (11);	$m$ ,	index for cosine term in heat-transfer relation;
$A$ ,	constant in heat-transfer relation, equation (6);	$M$ ,	Mach number;
$B$ ,	coefficient in heat-transfer relation, equation (6);	$n$ ,	index for incident flow speed in heat-transfer relation;
$d$ ,	diameter of cylindrical cross section;	$Nu$ ,	Nusselt number, based on fluid conductivity at free stream temperature;
$Gr$ ,	Grashof number;	$Pe$ ,	Péclet number;
$h_T$ ,	surface heat-transfer coefficient, a function of $T$ , averaged for the cross section;	$Pr$ ,	Prandtl number at free stream temperature;
$h_0$ ,	constant in equation for the heat-transfer coefficient;	$Re$ ,	Reynolds number, based on cylinder diameter;
$i$ ,	probe heating current;	$R_w$ ,	wire total electrical resistance;
$k_T$ ,	probe thermal conductivity, a function of $T$ ;	$T$ ,	wire local temperature; a function of $x$ ;
$Kn$ ,	Knudsen number ( $\lambda/d$ );	$T_0$ ,	ambient temperature;
$2l$ ,	total wire length;	$T_2$ ,	temperature of fluid incident to wire, a function of $x$ ;
$L$ ,	wire length to diameter ratio;	$x$ ,	position along the wire ( $x = 0$ at centre);
		$\alpha$ ,	thermal accommodation coefficient;

- $\beta$ , coefficient in equation for the heat-transfer coefficient;  
 $\gamma$ , ratio of specific heats of fluid;  
 $\varepsilon$ , surface emissivity of the probe surface;  
 $\lambda$ , molecular mean free path length;  
 $A$ , ratio of heat loss by conduction to the wire ends;  
 $\rho$ , resistivity of wire material;  
 $\sigma_0$ , Boltzmann's constant;  
 $\sigma_T$ , Thompson thermoelectric coefficient;  
 $\tau$ , nondimensional temperature based on resistance law for tungsten wires.

dealt with the well known half power law relating Nusselt ( $Nu$ ) and Reynolds ( $Re$ ) numbers for large Péclet numbers ( $Pe = Re \times Pr$ , where  $Pr$  = fluid Prandtl number). King also derived solutions for small Péclet numbers, his results being, for large Péclet numbers

$$Nu = 1/\pi + 2\sqrt{(Pe/\pi)} \quad (1a)$$

and for small Péclet numbers

$$Nu = \frac{2}{\log(1/Pe) + 0.423} \quad (1b)$$

## 1. INTRODUCTION

THE CALIBRATIONS of heated anemometer probes (usually operated at approximately constant temperature) depend primarily upon the relationships which exist between probe surface heat transfer rates and flow conditions over the probe. In addition to this loss of heat from the surface of an anemometer probe, the total measured power loss contains a significant component due to the conduction of heat into the probe mountings. King [1] and many subsequent investigators have used approximate solutions for the temperature distributions in the heated probe (a wire in most cases), from which the conductive heat loss to the supports could be estimated. Davies and Fisher [2] and others have introduced numerical solutions to the differential equation for the probe temperature distribution, since it was found that the approximate analytic solutions did not match all the required boundary conditions accurately due to the simplifying assumptions previously made. It is then possible to find satisfactory solutions in the more complicated situations, such as those where the conductive heat loss to the supports predominates over the surface heat loss or where the wire is yawed and the distribution of temperature becomes asymmetric. These solutions will be discussed further in the present paper.

1. (i) *Cooling of cylinders with normal flow*  
 The analyses of Boussinesq [3] and King [1]

More recently, Cole and Roshko [4] have derived the result for low Péclet numbers in a more accurate form, whilst Illingworth [5] includes a second order term in an expansion for the Nusselt number in terms of the Péclet number. The analysis at low Péclet numbers has been further refined using series solutions for the Oseen equations by Wood [6] and Hieber and Gebhart [7].

It may be seen from equation (1b) that, as the Péclet number becomes very small, the Nusselt number tends to zero. In practice, however, some lower limit for the Nusselt number exists due to the finite loss of heat measured in a stationary ambient fluid by natural convection and conduction in the fluid. This, therefore, places a severe restriction on the use of this relation as  $Pe \rightarrow 0$ . This limiting condition has been studied experimentally by Collis and Williams ([8] and [9]), whilst a theoretical discussion relating to the interaction of natural convective and conductive heat transfer to the fluid was given by Mahony [10]. Both of these works showed that natural convective flows were only a significant factor in the determination of the surface heat loss if the parameter  $L\sqrt{Gr}$  (where  $L$  is the length to diameter ratio of the wire and  $Gr$  is the Grashof number based on the diameter) exceeded unity. For smaller values of  $L\sqrt{Gr}$ , the heat transfer under static fluid conditions was determined solely by the conduction of heat through the fluid. Mahony

gave the following results for  $L\sqrt{Gr} > 1$ ,

$$Nu = -\frac{3}{\log_e Gr} \quad (2a)$$

and, secondly, for  $L\sqrt{Gr} < 1$ ,

$$Nu = \frac{1}{\log_e 2L} \quad (2b)$$

provided that the Grashof number itself remained small.

The non-linear dependence of the anemometer heat loss upon surface temperature, apart from variations introduced in the Grashof number, has received considerable experimental attention. Davies and Fisher [2] proposed that the heat transfer should be linearly related to the fluid thermal conductivity of the fluid at the probe surface temperature and reconciled this behaviour with their measurements with fine tungsten wires made in air at atmospheric pressure. They also suggested that the index relating the Reynolds and Nusselt numbers in the range  $R < 44$  had a value closer to  $\frac{1}{3}$  rather than  $\frac{1}{2}$  as derived by King. Previously, McAdams [11] and Douglas and Churchill [12], amongst others, evaluated the fluid viscosity and conductivity at the arithmetic mean of the wire and ambient temperatures in order to reduce the results at different overheat ratios to a common relationship between the Nusselt and Reynolds numbers. The nonlinear effect of probe temperature is quite significant as the temperature of the probe can exceed  $400^\circ\text{C}$  in gases and the corresponding ratio of properties, such as viscosity and conductivity, at the surface and in the ambient fluid can be large. Whilst the correlations for the various sets of data mentioned have been made on the basis of the fluid properties at either ambient, arithmetic mean or logarithmic mean temperatures, it appears that the suitability of each type of average will depend upon the Péclet number and magnitude of the variation of fluid conductivity. For example, as  $Pe \rightarrow 0$  the fluid heat transfer becomes conductive close to the wire and a logarithmic

mean should be selected. Again, for small temperature differences a linear average could be adequate. In general, it appears preferable to introduce the overheat ratio or surface temperature as an additional independent variable.

Comparison of measurements at different gas flow densities introduces the effect of the Knudsen number ( $Kn = \lambda/d$ , where  $\lambda$  = molecular mean free path and  $d$  = probe diameter), which can be used to find the flow Mach number for any given Reynolds number from the relationship

$$M = ReKn\sqrt{(2/\gamma\pi)} \quad (3)$$

where  $\gamma$  = ratio of specific heats of the gas. It follows that only two of these parameters are needed to specify the flow. The Mach number is omitted as a separate independent variable in the present paper, since all the experiments were conducted with  $M < 0.5$ .

The majority of reported heat transfer measurements for anemometers in variable density slip flows have been made with  $Re > 2$  and have been reviewed by Baldwin [13] and by Baldwin, Laurence and Sandborn [14]. Analyses of slip flow heat transfer from circular cylinders have generally been restricted to subsonic flow, introducing a modified temperature boundary condition at the surface to an assumed continuum external flow in order to provide a simple model for analysis. This approach has been adopted by Sauer and Drake [15] (using numerical solutions) and Levy [16] amongst others. The predicted heat transfer rates are found to deviate quantitatively from the measured data, such as that of Winovich and Stine [17] or Spangenberg [18]. The general trend of the relationship between Nusselt, Knudsen and Reynolds numbers is, however, predicted correctly, there being a progressive reduction of Nusselt number with increasing Knudsen number.

Theoretical analyses are well developed for

free molecular flow at large Knudsen numbers (for example, the analyses of Stalder, Goodwin and Greager ([19, 20]), Oppenheim [21] and Bell and Schaaf [22]), the most significant uncertainty being the value of the surface thermal accommodation coefficient ( $\alpha$ ). This has been found to depend strongly upon the surface condition and Wachman [23] and Schaaf [24] have reported variations in the available data for between 0.02 and unity for tungsten. With zero incident flow speed Madden and Piret [23] derived the following relationship for all Knudsen numbers:

$$2/Nu = 2/Nu_c + \frac{8\gamma}{\alpha Pr(\gamma + 1)} \left( \frac{\lambda}{d} \right) - \log_e(1 + 2\lambda/d). \quad (4)$$

The parameter  $Nu_c$  may be regarded as the continuum static condition Nusselt number and was represented by Madden and Piret in terms of a diameter  $b$  around the circular cylinder at which the temperature was equal to ambient temperature. It is evident that  $Nu_c$  would have to correspond to the Nusselt numbers given by equations (2a) and (2b) as appropriate.

#### 1. (ii) *Cooling of cylinders yawed to the incident flow*

When anemometer probes are yawed at some incidence to the flow, the heat loss is modified due to the change of incident mass flux at the probe (reduced by the cosine of the yaw angle), the change from circular to an elliptical cross section and the introduction of three-dimensional effects along the whole probe. The use of suitable trigonometric calibration laws at large Péclet numbers has been discussed by Sandborn and Laurence [26], and Baldwin, Laurence and Sandborn [14], who correlated experimental measurements on the basis of the normal component of velocity to the probe. Webster [27] used the following expression as suggested by Hinze [28]:

$$Nu = A + B\sqrt{u_e} \quad (5)$$

with

$$u_e = u_0(\cos^2 \theta + a^2 \sin^2 \theta)^{\frac{1}{2}}$$

where  $u_0$  = incident flow speed and  $\theta$  = yaw angle.

The constant  $a$  was found to have a value of 0.2, being introduced to allow for the finite heat loss when the flow was parallel to the wire. This relationship has been treated in more detail by Freije and Schwarz [29] who constructed a suitable expression for  $a$  to match their measurements made with fine wires and cylindrical film probes, the latter operating at  $Re > 44$  where eddy shedding would occur in the cylinder wake. Champagne [30] showed that the coefficient  $a$  could be related empirically to the wire aspect ratio ( $L$ ) in his investigation of the calibration laws. He also measured the distribution of temperature along the wire by an infra red technique. At a yaw angle of  $55^\circ$  his results indicated a slight asymmetry with a downstream shift of the peak temperature as might be expected.

From this discussion it may be seen that a number of different factors influence the loss of heat from anemometer probes and that they will under certain conditions combine in a complicated manner to determine the heat transfer rate. It is one aim of the present paper to present results which lie in the transition regions between the regime of dominance of the individual heat-transfer mechanisms, as well as to develop more fully the application of numerical methods to solve for the thermal equilibrium of the probe. In particular, this latter aspect enables measurements to be made where the surface heat flux to the fluid is relatively low in relation to the conduction to the supports, and also permits a solution of the asymmetric cooling problem.

#### 2. HEAT TRANSFER FROM CYLINDRICAL PROBES WITH FLOW NORMAL TO THE CYLINDER AXIS

The overall nature of the calibration of a constant temperature anemometer is illustrated

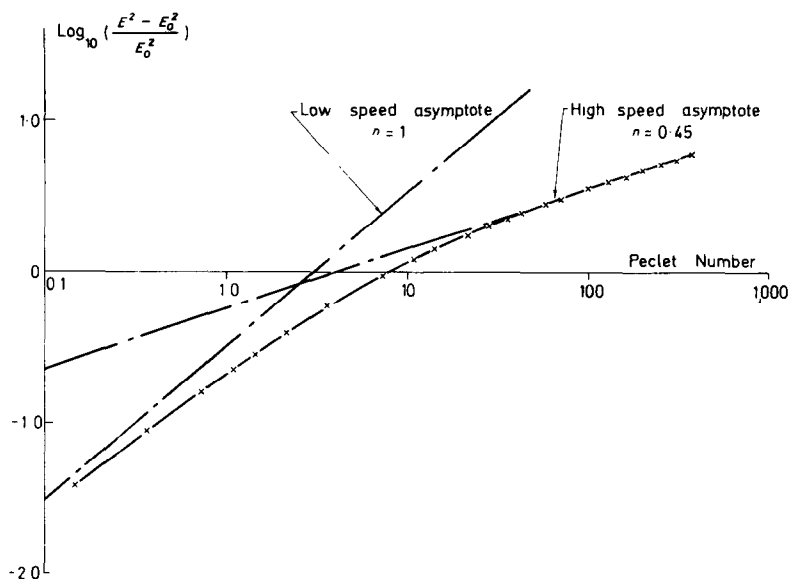


FIG. 1. Calibration of a hot wire probe at atmospheric pressure.

Wire length = 2 mm Resistance =  $14.97 \Omega$   
Diameter =  $5.1 \times 10^{-4}$  cm

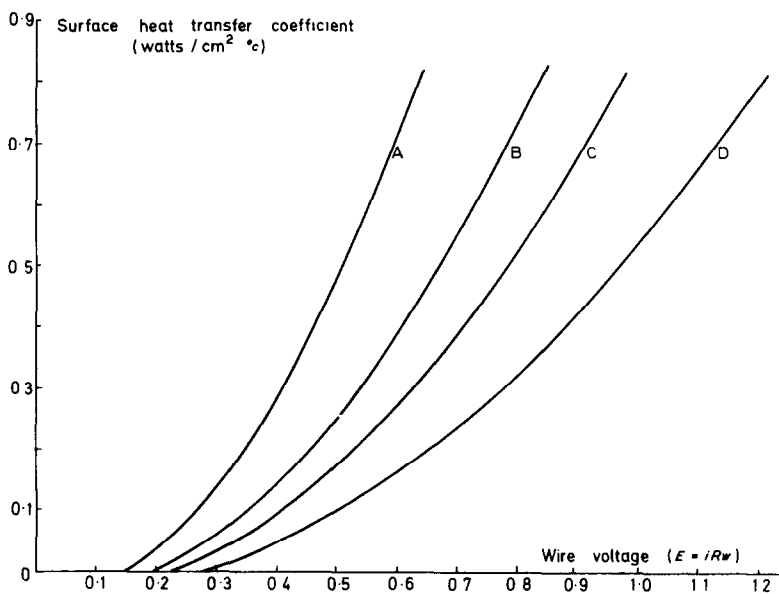


FIG. 2. Computed relationship between surface heat-transfer coefficient and heating current.

Wire length = 0.184 cm Diameter =  $5.1 \times 10^{-4}$  cm

A:  $R_w = 9.62$ ,  $T_{av} = 168^\circ\text{C}$

B:  $R_w = 11.35$ ,  $T_{av} = 240^\circ\text{C}$

C:  $R_w = 12.66$ ,  $T_{av} = 283^\circ\text{C}$

D:  $R_w = 14.97$ ,  $T_{av} = 383^\circ\text{C}$

by the series of experimental measurements shown in Fig. 1. The presentation adopted is intended to show the calibration in relation to a general law of the form

$$Nu = A + BRe^n \quad (6)$$

where  $A$ ,  $B$  and  $n$  are constants. The constant  $A$  will, of course, include the effects of conduction to the supports and the finite heat loss rate at zero Reynolds number. It may be seen that there is a departure from a single law (approximating to  $n = 0.45$ ) at the larger Péclet numbers, the index  $n$  approaching unity as the Péclet number becomes small. For this particular probe the parameter  $L\sqrt{Gr}$  was less than unity and so no effects due to natural convective flows were observed as  $Pe \rightarrow 0$ , the wire current calibration approaching the intercept uniformly as  $Pe \rightarrow 0$ . Thus the low Péclet number calibrations appear to take the form of a linear perturbation of the total heat loss from the zero flow value. The change in the calibration takes place in the range  $0.1 < Pe < 10$ , and thus corresponds to a transition from a predominantly fluid conductive surface cooling situation. The deviation of the index  $n$  from the value 0.5 in the range  $Pe > 10$  has been discussed by Collis and Williams [31], Sandborn and Laurence [26] and Delleur [32], and may be attributed to the finite length and temperature loading effects experienced in practice. Previous authors have extended the range over which the relationship of equation (6) approximates their data by selecting a value of  $E_0$  (Fig. 1) which differs from the value obtained at zero Reynolds number. However, it is evident that this method cannot encompass a calibration which approaches  $Re = 0$  closely. It should also be borne in mind that the representation of an overall heat loss calibration by equation (6) includes the conduction of heat to the supports. Hence, the values of the constants introduced may not necessarily correspond to those on the basis of the surface heat-transfer process alone.

When the surface heat-transfer rate is small, the interpretation of the total power loss measurement requires the accurate solution of the thermal

equilibrium equation so that the conductive heat transfer to the supports and other heat loss terms are accurately estimated. Davies and Fisher [2] pointed out deficiencies in the use of approximate analytic solutions of the type introduced by King [1] and used subsequently by many others, such as Lowell [33]. Accordingly, they adopted a numerical integration method to solve the equation for thermal equilibrium, enabling all the temperature dependent properties of the wire to be included. This method is also used in the present work, the differential equation for the wire temperature ( $T$ ) as a function of position ( $x$ ) along the wire carrying current ( $i$ ) being as follows:

$$\frac{\pi d^2}{4} \frac{d}{dx} \left( k_T \frac{dT}{dx} \right) + \frac{4i^2}{\pi d^2} \rho_T - \pi d h_T (T - T_0) - \varepsilon_T \sigma_0 \pi d (T^4 - T_0^4) + \sigma_T i \frac{dT}{dx} = 0 \quad (7)$$

where  $k_T$ ,  $\rho_T$  and  $h_T$  are the temperature dependent thermal conductivity, resistivity and surface heat-transfer coefficient of the wire of diameter  $d$ . The Thompson thermoelectric coefficient is  $\sigma_T$ , and  $\varepsilon_T$  denotes the surface radiation emissivity,  $\sigma_0$  being Boltzmann's constant. The incident fluid and surroundings have a temperature  $T_0$ ,  $h_T$  being an average coefficient for the circular cross section. Solutions are found to equation (7) by iterating for the unknown heat-transfer coefficient  $h_T$  and the temperature gradient  $(dT/dx)_{x=-l}$  in terms of the wire total electrical resistance and the temperature  $(T)_{x=+l}$  respectively. All the other terms in equation (7) are measured or else assumed to have the properties which are available for tungsten. In this way a wire calibration relating surface heat-transfer coefficient to the heating current can be built up from individual solutions. The form of such a calibration is shown in Fig. 2 for a particular tungsten wire.

The heating current required to maintain the probe resistance (i.e. average temperature) at the required level with zero convective surface heat transfer (i.e. when mounted in a sufficiently low

vacuum) is determined only by the geometry and properties of the wire. Thus it is possible to match the experimentally measured heating current under vacuum conditions around the wire to the current calculated from equation (7) for this condition by making adjustments to the wire properties and geometry until the two heating current values correspond. The iterative procedure thus adopted was to iterate for the wire properties (that is,  $\rho_T$ ,  $k_T$ , etc.) using the experimentally measured value of  $i$  with  $h_T = 0$  in equation (7). It was found that errors of less than 0.5 per cent resulted in the computed wire resistance, obtained by integrating numerically along the wire, for these cases.

For the experimental measurements made with a series of tungsten wires it was found that the properties stated in Table 1 most nearly satisfied all the different vacuum heating results, and that the zero surface cooling case for any individual wire could be matched by making variations in resistivity of  $\pm 2$  per cent from the

values given in Table 1. A further discussion of the selection of material properties was given by Davis and Davies [34], when it was concluded that the nominal value for  $k_T$  for tungsten should be used and that the resistivity law should be modified so as to most nearly match all the wires tested. Care was maintained in selecting wires, rejecting those which gave a current more than 0.5 per cent below the required value for the wire length, as this was interpreted as indicating an increase in cold resistance due to physical damage. The wires selected thus required a heating current close to the maximum for the whole set (of over 200 wires), taking account of the wire length. Due to cancellation of effects it was found that the variation of the resistivity  $\rho_T$  required from one wire to another would introduce a corresponding uncertainty of  $\pm 2$  per cent in the calculated heat-transfer coefficient provided the selected properties always matched the experimental heating conditions in a vacuum. A vacuum of 0.002 torr was found to be adequate to establish an effectively zero surface heat-transfer environment, as no change of overall heat loss was observed when the pressure was increased until a pressure of 0.010 torr was reached.

In order to simplify the iteration for the unknown  $h_T$  and the temperature gradient  $(dT/dx)_{x=-l}$  in integrating equation (7), the following approximate overall heat balance equation was introduced to relate these two unknown quantities:

$$i^2 R_w = 2l\pi d h_{av} (T_{av} - T_0) K + 2k_0 \cdot \frac{\pi d^2}{4} \left( \frac{dT}{dx} \right)_{-1} \quad (8)$$

where  $R_w$  = wire resistance,  $2l$  = wire length and average values of wire temperature ( $T_{av}$ ) and heat-transfer coefficient ( $h_{av}$ ) are introduced. The factor  $K$  as introduced in equation (8) is only approximate and varied only between 1.0 and 1.15 for these symmetric solutions. The iteration for  $K$  and  $h_{av}$  was found very sensitive to the value for  $h_{av}$ , and for cases where the

Table 1. Properties of tungsten wire material

#### Resistivity

$$\rho_T = 10^{-6} \times \left[ \rho_0 + \rho_a \left( \frac{T-54}{237} \right) + \rho_b \left( \frac{T-54}{237} \right)^2 \right] \Omega \text{ cm}$$

where  $T$  is the temperature in degrees Kelvin.

Nominally pure tungsten:  $\rho_0 = 0$ ,  $\rho_a = 5.2$ ,  $\rho_b = 0.21$

Values selected to match experimental heat loss data measured under vacuum conditions:

$$\rho_0 = 1.2, \rho_a = 5.0, \rho_b = 0.20$$

#### Thermal conductivity

$$R_T = 6.92 \times \left( \frac{T}{\rho_T} \right) \times 10^{-6} \text{ W(cm)}^{-2} (\text{°K})^{-1}$$

#### Emissivity of tungsten surfaces

$$\varepsilon_T = -0.012 + 1.11 \times 10^{-4} T$$

#### Thompson coefficient for tungsten

$$\sigma_T = 3.4 T \times 10^{-8} \text{ V/°K}$$

#### Wire diameter

$$d = 5.1 \times 10^{-4} \text{ cm}$$

surface heat loss exceeded the conductive loss to the supports it was found that  $h_{av}$  had to be evaluated to as many as 9 decimal places to match the  $T_{x=+l}$  boundary condition to  $\pm 2^\circ\text{C}$ . This was due to the dominance of the convective term in equation (8), where  $(dT/dx)_{-l}$  is evaluated as the difference of the other two terms and as a result an increase in the value taken for  $h_{av}$  decreased the value of  $(T)_{x=+l}$  obtained in the solution. For cases of lower surface cooling the effect was not as severe, and where the convective loss was the smaller term in equation (8) the value of  $h_{av}$  assumed was most significant where it appeared in equation (7) during integration, as the effect of an increase in the assumed value of  $h_{av}$  then resulted in an increase

in the value of  $(T)_{x=+l}$  obtained; i.e. the sense of the iteration had to be reversed. Where the convective and conductive (support) losses were nearly equal the iteration became complicated as two solutions could be found for  $h_{av}$ , only one of which satisfied the resistance integral condition. The solution at the boundary between these two iterative regions was found to have only a single solution as the solution moved from one limb of the curve  $(T)_{x=+l} = f(h_{av})$  to the other, the curve having a maximum value between the two limbs.

The application of the calibration of Fig. 2 to a series of measurements made with the same wire is shown in Fig. 3, the wire being mounted in the potential core of a variable density convergent nozzle operated by a suction pumping system. The strong dependence of the Nusselt number on Knudsen number is seen to be more marked for the higher Reynolds number cases, where no

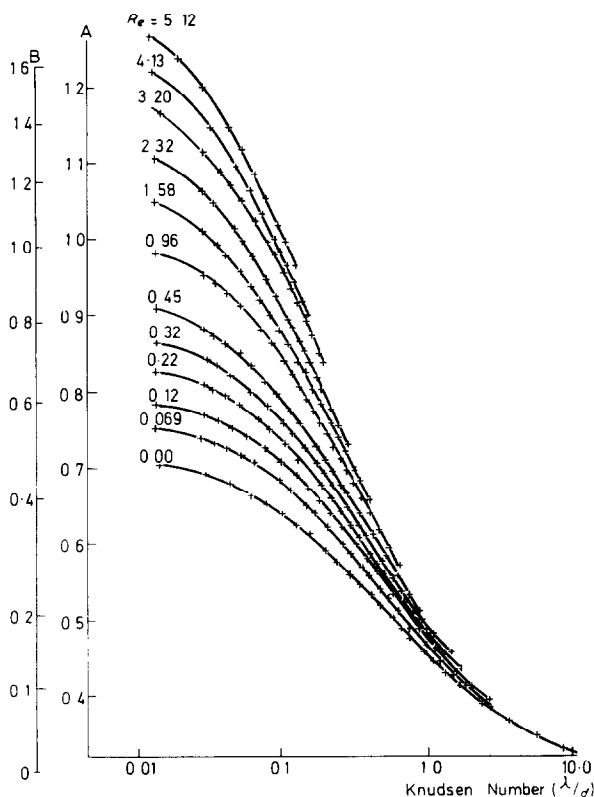


FIG. 3. Heat transfer from a hot wire probe operated in a variable density subsonic airstream.

Wire length = 0.194 cm Resistance = 14.97  $\Omega$

Diameter =  $5.1 \times 10^{-4}$  cm

Scale A: Wire voltage Scale B: Surface Nusselt number

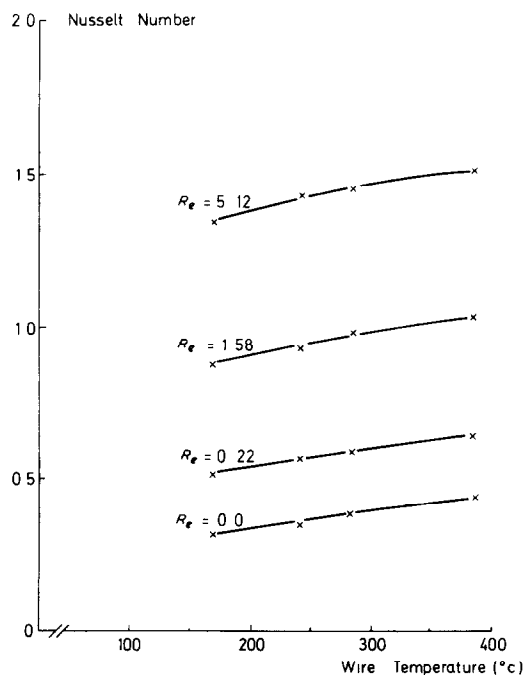


FIG. 4. Dependence of surface heat-transfer coefficient upon surface temperature.

Wire length = 0.194 cm Diameter =  $5.1 \times 10^{-4}$  cm

Knudsen number = 0.05.



close approach to continuum conditions is found for the range of Knudsen numbers covered. At the lower Reynolds numbers, however, the Nusselt number has become almost independent of Knudsen number when  $Kn < 0.01$ . The results for the Nusselt number were found to be temperature dependent, as may be seen from Fig. 4 where the measurements at a fixed Knudsen number but for varying wire average temperature are shown. In making the calculations described above, the local heat-transfer coefficient ( $h_T$ ) has been assumed to be constant, independent of the local wire temperature and thus equal to the average heat-transfer coefficient ( $h_{av}$ ). The dependence of the Nusselt number upon temperature obtained from Fig. 4 was subsequently used to form a linear empirical expression for  $h_T$ , of the form  $h_T = h_0(1 + \beta(T - T_0))$  as used by Davies and Fisher [2]. However, repeating the numerical solutions including this relationship was not found to alter the result significantly

for the average heat-transfer coefficient shown in Fig. 4, and it was concluded that, for the relatively small variation with the temperature shown by these results, the approximation of assuming a constant value for  $h_T$  during numerical integration introduced no significant errors.

The experimental results may be compared with the theoretical results of Sauer and Drake [15] shown in Fig. 5. The experimental Nusselt numbers are seen to rise much more rapidly with Knudsen number, and it can be seen that this effect is more pronounced at the higher wire temperature. As will be mentioned in the following paragraphs, the heat-transfer coefficient is found to be independent of wire temperature under free molecular flow conditions, and it thus appears that there is a progressively increasing temperature dependence with decreasing Knudsen number in the slip flow region. The temperature dependence of the Nusselt number in continuum flow is thus approached smoothly

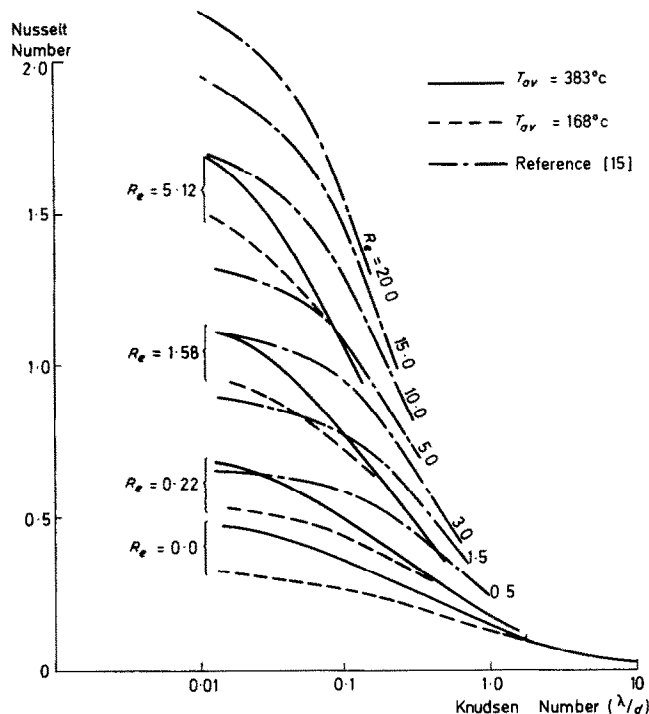


FIG. 5. Comparison between experimental results and the computed data of Sauer and Drake [15].

from the free molecular situation by this steady increase. Hence the non-linear behaviour of the heat transfer makes a close comparison between experiment and theory more difficult.

The results shown in Figs. 3–5 all include the

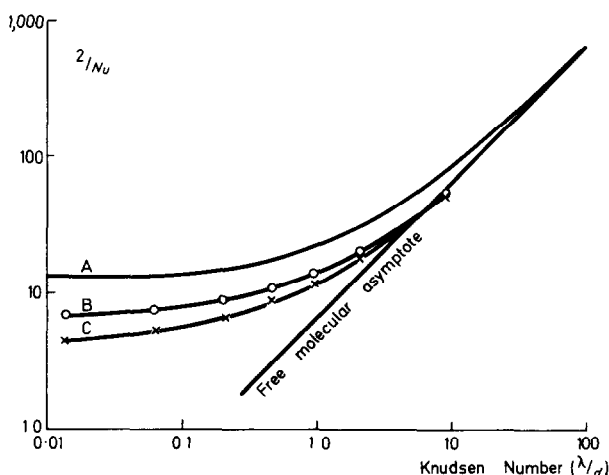


FIG. 6. Heat transfer with no incident flow.  
Wire length = 0.24 cm Diameter =  $5.1 \times 10^{-4}$  cm  
A: Equation (4) B:  $T_{av} = 70^\circ\text{C}$  C:  $T_{av} = 380^\circ\text{C}$ .

limiting case  $Re = 0$ , and it is found that similar temperature and Knudsen number effects are present for this condition as for the forced cooling conditions. The results are compared with equation (4) in Fig. 6, from which it may be seen that the experimental Nusselt numbers are considerably larger than the prediction of equation (4). The expression used for  $Nu_c$  in this equation is of the form given by equation (2b), since natural convective effects were not observed as the wire was rotated in relation to the vertical direction. The parameter  $L\sqrt{Gr}$  had a value of 0.8, confirming this observation. Solutions for the thermal equilibrium of the wires at this condition showed that the surface heat loss to the fluid was still approximately 75 per cent of the overall heat loss and thus any variation of the surface heat loss with wire orientation would be detected in the total power loss measurement. From Fig. 6 it may be seen that the experiments deviate significantly from equation (4) as continuum conditions are approached, although the general form of the transition to free molecular behaviour is correct. A good fit to the experi-

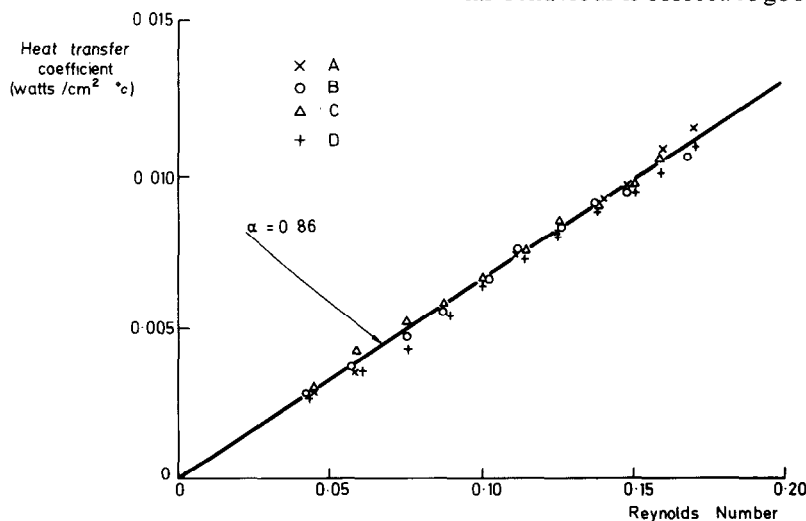


FIG. 7. Heat transfer from a hot wire probe in free molecular flow.

Wire length = 0.19 cm Diameter =  $5.1 \times 10^{-4}$  cm  
A:  $R_w = 9.62\Omega$ ,  $T_{av} = 160^\circ\text{C}$   
B:  $R_w = 11.35\Omega$ ,  $T_{av} = 243^\circ\text{C}$   
C:  $R_w = 12.66\Omega$ ,  $T_{av} = 300^\circ\text{C}$   
D:  $R_w = 14.97\Omega$ ,  $T_{av} = 393^\circ\text{C}$ .

mental data may in fact be obtained by modifying the value of  $Nu_c$  in equation (4), although some considerable part of the observed discrepancies is due to the effect of wire temperature. The close proximity of the hot wire supports to the wire would also be expected to modify the heat loss rates, and it seems that this has caused the experimental Nusselt numbers to be larger than expected due to the presence of cold surfaces close to the wire.

Under conditions of free molecular flow, the surface heat-transfer coefficient was found to be independent of surface temperature, as illustrated by Fig. 7 where a 5 micron wire was mounted in a sonic low density jet, the mass flow rate being controlled by varying the stagnation pressure. The Stanton numbers calculated by

Oppenheim [21] were used to calculate the accommodation coefficient corresponding to the best line through the data, a value of  $\alpha = 0.86$  being obtained for the tungsten wire in air. Due to the small magnitude of the surface heat transfer, the measurements were made by accurately measuring the increase of heating current over the heating current in a low vacuum, no adjustments being made to the anemometer system between the two readings. Similarly, the heat-transfer coefficients were calculated by accurately matching the vacuum heating equilibrium condition by a suitable adjustment of the wire properties and then calculating the heat-transfer coefficients for small increases in the heating current.

The measurements discussed in the preceding

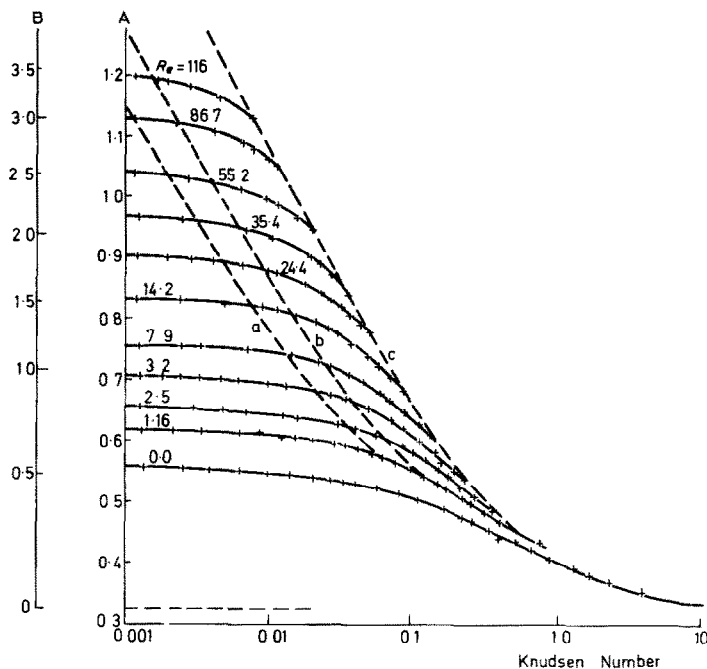


FIG. 8. Heat transfer from a cylindrical thin film probe operated in a variable density subsonic airstream.

Diameter of quartz coated film element =  $5.3 \times 10^{-3}$  cm  
Resistance (cold) =  $7.42 \Omega$ . Length of resistance element =  $0.106$  cm. Resistance (hot) =  $11.57 \Omega$ .

Scale A: Probe voltage      Scale B: Surface Nusselt number

a: Mach number = 0.05      b: Mach number = 0.1,

c: Mach number = 0.5.

paragraphs have all been made using fine tungsten wires. Figure 8 illustrates a similar subsonic slip flow calibration for a cylindrical quartz probe, coated with a thin platinum film and with an overall protective coating of quartz deposited by a radio-frequency sputtering method. This probe was supplied by Thermo-Systems Inc., of Minneapolis-St. Paul, Minnesota. The increased size of this probe has reduced the operating range of Knudsen numbers by an order of magnitude, the measurements having been made for an identical range of pressure and flow rates as in Fig. 3. A subsidiary, non-linear scale for the probe Nusselt number has been calculated for Fig. 8 on the assumption that the heat loss by assumption that the heat loss by conduction to

the substrate and supports remained constant. This loss by conduction only was measured directly, with the probe mounted in a vacuum chamber as for the hot wire experiments. The assumption that the loss of heat by conduction to the substrate remains constant will clearly introduce some errors into the calculated Nusselt numbers, although these should be no worse than for the case of a hot wire since the effect of the larger probe diameter is largely offset by its lower thermal conductivity, the factor  $[k_0(\pi d^2/4)]$  for the quartz probe being 46 per cent of that for a 5 micron tungsten wire. Further uncertainties are introduced by the gold painted connecting sectors of the quartz cylinder to either side of the heated film, which will become heated and

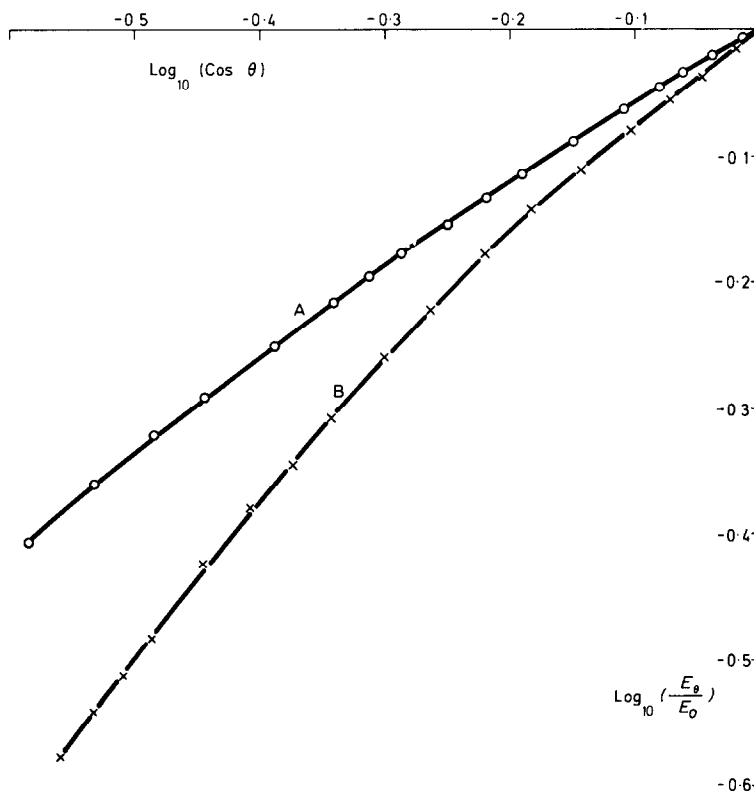


FIG. 9. Calibration of a hot wire probe as a function of yaw angle.

Wire length = 0.24 cm      Resistance = 18.1  $\Omega$

Diameter =  $5.1 \times 10^{-4}$  cm

A: Péclet number = 8.6

B: Péclet number = 0.76.

thus lose heat to the flow as well as modify the temperature at the ends of the film. Since the results of Fig. 8 demonstrate the general behaviour of the film probe adequately, full solutions for the thermal equilibrium of the probe have not been carried out in this case. However, the results shown in Fig. 8 demonstrate that the larger thin film probe is much less sensitive to pressure changes than is a hot wire probe at similar flow conditions due to its lower operating Knudsen number range.

### 3. HEAT TRANSFER FROM HOT WIRE PROBES WHEN YAWED TO THE INCIDENT FLOW DIRECTION

Although it is possible to use a number of methods for correlating the data obtained from the calibration of yawed hot wire probes, the results presented in Fig. 9 have been reduced in order to show the wire response in relation to the approximate heat-transfer law corresponding to equation (6) for a yawed wire. Allowing for some variation between the effects of yaw and speed due to flow along the wire, the form chosen is

$$Nu = A + B' V^n \cos^m \theta \quad (9)$$

where  $V$  is the speed of the incident flow and  $\theta$  is the angle between the flow direction and a line normal to the cylinder axis. Two indices  $m$  and  $n$  are chosen so as to permit a limited discrimination between the effects of speed and yaw, and a constant  $B'$  is introduced. From Fig. 9 it may be seen that the index  $m$  has a value of 0.6 at a probe Péclet number (based on the cylinder diameter) of 8.6, whilst at a lower Péclet number ( $Pe = 0.76$ ) the index  $m$  has a value of 0.81. These values apply for the slope of the yaw calibration at  $\theta = 45^\circ$ . It appears that there is a tendency for  $m$  to increase slightly with increasing yaw angle, particularly at the lower Péclet number where it appears that  $m$  varies in the range  $m > 0.75$ . The data on which Fig. 9 was based were taken at  $1^\circ$  intervals of yaw angle for a full range of  $-190^\circ < \theta < +190^\circ$ . This enabled the flow direction to be determined from the hot

wire calibration. Five readings of wire voltage were taken at each position using an automatic digital data recording system, the average of these being used as the basis for the values indicated by Fig. 9.

The extent to which three-dimensional flow effects give rise to an asymmetric response of the hot wire probe can be measured in terms of the ratio of the heat losses by conduction to the upstream and downstream supports. This ratio can be measured experimentally by mounting a thermocouple at the tip of one of the supports, the heat loss to the support being proportional to the indicated temperature rise. The ratio of upstream to downstream conductive end losses to the supports is simply obtained by rotating the probe through  $180^\circ$  so that the thermocouple is successively at each position. In practice it is also necessary to measure the thermoelectric signal as the average of two values with the wire heating current reversed in direction, since there was generally a significant voltage generated in the thermoelectric circuit by the heating current at the position where the thermocouple was soldered to the probe. This current reversal also causes the Thompson effect term in the equilibrium equation to be eliminated on the average of the two readings and, since the effect was found to be small (giving rise to less than 5 per cent difference between the heat loss from the ends of a 2 mm tungsten wire, 5 mm in diameter), the term has not been included for the solutions reported here. The Thompson heating term had a negligible effect on the overall balance of energy, as it averages to zero over the wire length.

It may be seen that equation (7) is of the form

$$\frac{d^2 T}{dx^2} = f \left[ T, \left( \frac{dT}{dx} \right)^2 \right] \quad (10)$$

if the Thompson effect is omitted and hence solutions will always be symmetric about points of maximum temperature. To introduce asymmetry into the solution, some modification to the surface heat-transfer term is required, since it is due to the effects of the flow that asymmetry

occurs. The simplified model which is now introduced allows the fluid incident temperature to vary along the wire, replacing  $T_0$  in the convective term by  $T_2(x)$ . This then represents the heating of the flow at upstream sections of the wire before passing over downstream sections,  $T_2(x)$  increasing with  $x$ . Where the flow is not parallel to the wire, these increases will arise due to the diffusion of heat at right angles to the streamlines. From this it is expected that the magnitude of the increase in  $T_2(x)$  along a yawed wire will be greater at small Péclet numbers, as the factor  $(1/Pe)$  determines the extent of heat diffusion across the streamlines. In order to find a solution for  $T_2(x)$ , it is assumed that the rate of increase of  $T_2(x)$  is proportional to the local heat transfer from the wire to the flow. That is

$$\frac{dT_2}{dx} = a_1 \pi d h_T (T - T_2) \quad (11)$$

where  $a_1$  is a constant of proportionality. This differential equation for  $T_2(x)$  is solved together with a modified equilibrium equation for the wire,

$$\frac{\pi d^2}{4} \frac{d}{dx} \left( k_T \frac{dT}{dx} \right) + \frac{4i^2 \rho_T}{\pi d^2} - \pi d h_T (T - T_2) - \varepsilon_T \sigma_0 \pi d (T^4 - T_0^4) = 0. \quad (12)$$

The coefficient  $a_1$  is the only additional unknown introduced into these asymmetric equations and is determined iteratively by matching the solution for  $T(x)$  to the required ratio ( $A$ ) of end losses, where

$$A = \left| \frac{(dT/dx)_{+l}}{(dT/dx)_{-l}} \right|. \quad (13)$$

The iterations for the heat transfer coefficient and correction factor  $K$  proceeded as for the symmetric solutions, except that the average energy balance equation was modified to become

$$i^2 R_w = K \cdot \pi d \cdot 2l h_{av} (T_{av} - T_{2av}) + (1 + A) k_0 \times \frac{\pi d^2}{4} \left| \left( \frac{dT}{dx} \right)_{-l} \right|. \quad (14)$$

Solutions were carried out with  $A > 1$ , so that  $x = -l$  corresponded to the upstream end of the wire. Estimates of the average fluid temperature  $T_{2av}$  were based on the approximate average equation

$$\frac{T_{2av} - T_0}{2l} = \frac{a_1 \pi d h_{av} (T_{av} - T_{2av})}{2} \quad (15)$$

which, when re-arranging to give an expression for the average fluid temperature, becomes

$$T_{2av} = T_0 + \frac{T_{av} - T_0}{\{1 + 1/(\pi d h_{av} l a_1)\}}. \quad (16)$$

The value of  $T_{2av}$  may then be substituted into equation (14). It was found that the correcting factor  $K$  still lay in the range  $0.95 < K < 1.15$  in spite of this additional approximation. The iterations for the unknown  $K$  and  $a_1$  were made to converge more rapidly by linear interpolation for the former in terms of the integrated resistance of any solution for  $T(x)$  and for the latter in terms of the ratio  $A$ . There was not found to be any strong interaction between these iterations, the most difficult part of obtaining any solution still being the determination of the heat transfer coefficient to the eight or nine significant figures required to generate the temperature gradient  $(dT/dx)_{-l}$  from equation (14) with sufficient precision to match the boundary condition  $T(+l)$  to the required accuracy.

Solutions obtained for two different incident flow speeds on the basis of the measured values of the ratio  $A$  are shown in Fig. 10. It can be seen that a significant asymmetry in the distribution of temperature only occurs at large angles of yaws in excess of  $70^\circ$ , the maximum downstream shift in the location of the peak temperature being approximately 30 per cent of the wire length from the centre in each case. A comparison of the results shown in Figs. 10a and 10b shows that the asymmetric effects are confined to a smaller range of yaw angles near to parallel flow at the higher Péclet number. This effect would be expected on the basis of a smaller cross-flow diffusion of heat at the higher Péclet number.

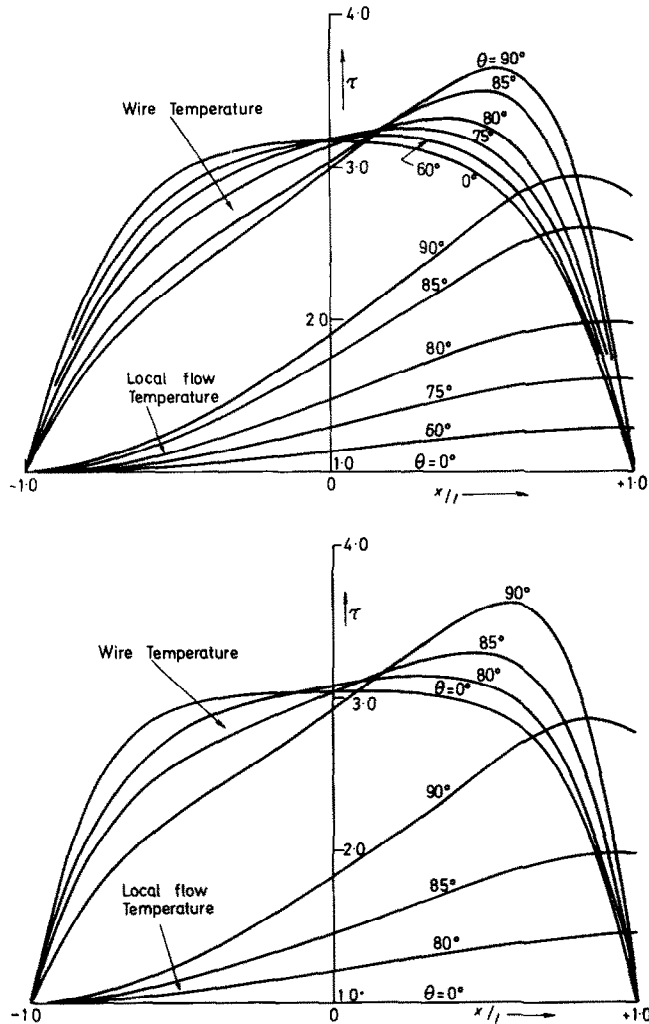


FIG. 10. Distribution of temperature along a yawed wire computed from asymmetric and loss data.  
 Wire length = 0.17 cm      Resistance = 14.75  $\Omega$   
 Diameter =  $5.1 \times 10^{-4}$  cm  
 (a) Péclet number = 1.4      (b) Péclet number  $\approx 11.3$ .

Values of the measured ratio and the coefficient  $a_1$  corresponding to these solutions are given in Table 2, where it is seen that the surface heat-transfer coefficient at high yaw angles increases quite significantly instead of continuing to decrease with a yaw as might be expected from the application of a cosine law to the measured total power loss. For these experiments with air

flowing over a fine wire, with a Prandtl number of order unity, it would be expected that the onset of significant three-dimensional flow effects would correspond to the development of a significant three-dimensional temperature effect around the wire, as represented by  $T_2(x)$ . In consequence, the change of behaviour of the heat-transfer coefficient, which would depend upon

Table 2. Measurements with yawed wires  
Wire length = 0.17 cm Resistance = 14.75

Incident flow speed (m/s)	Yaw angle ( $\theta^\circ$ )	Wire voltage $E = iR$ (V)	End loss ratio $A$	Heat-transfer coefficient (average value) (W/cm <sup>2</sup> °C)	Asymmetric factor $a$ (°C/W)
4.88 ( $Pe = 1.07$ )	0	1.00	1.00	0.530	0
	30	0.98	1.04	0.516	320
	45	0.96	1.09	0.503	715
	60	0.93	1.17	0.487	1441
	75	0.89	1.39	0.483	3377
	80	0.88	1.72	0.538	5614
	85	0.87	2.52	0.673	9425
	90	0.86	3.20	0.782	11810
42.1 ( $Pe = 9.2$ )	0	1.34	1.00	1.015	0
	30	1.32	1.02	0.993	72
	45	1.28	1.04	0.938	149
	60	1.23	1.08	0.871	327
	75	1.13	1.16	0.749	797
	80	1.10	1.30	0.747	1509
	85	1.07	1.80	0.838	3583
	90	0.99	3.20	1.030	8217

the flow over the wire, would be expected to correspond with the occurrence of asymmetry, as has been measured. Further, the development of a three-dimensional flow over the wire would introduce a departure from the simple cosine behaviour of the probe Nusselt number, the Reynolds number characterizing the flow increasing as the situation changes towards a slender rather than a bluff body type of flow. The heat-transfer coefficient would be expected to vary along the wire at high yaw angles, with larger values near to the upstream end which would contribute to the downstream shift of the peak temperature. However, in view of the difficulty in setting up even an approximate model for the variation of heat-transfer coefficient, due to uncertainties in the upstream end flow boundary condition as well as the problem of flow past a sharply yawed cylinder, the results presented have been based on a constant heat-transfer coefficient along the wire.

The temperature dependence of the heat-transfer coefficient has been included in these solutions, although it has no great influence on the overall average results as discussed in

section 2. The form  $h_T = h_0\{1 + 2.0[(T - 54/237)]\}$  proposed by Davies and Fisher [2] has been used, although the results of section 2 might suggest a rather smaller temperature dependence of the heat-transfer coefficient. From the results it is seen that the measured heat loss continues to reduce with yaw angles due to the counteracting effect of the reduced average temperature difference ( $T_{av} - T_{2av}$ ) on the increased heat-transfer coefficient at high yaw angles.

A simple visual confirmation of the occurrence of asymmetric temperature distributions can be obtained by heating the wire above the oxidation temperature for the metal of which the wire is made. The resulting surface oxidation pattern may be used to locate the point of maximum temperature and to estimate qualitatively the distribution of temperature along the wire. With a tungsten wire a white oxide material is formed and usually penetrates the wire leading to a fracture at the point of maximum temperature. Figure 11 shows two wires which have been fractured in this way; with the flow normal to the wire the fracture was located centrally, whilst with the flow parallel to the wire the point



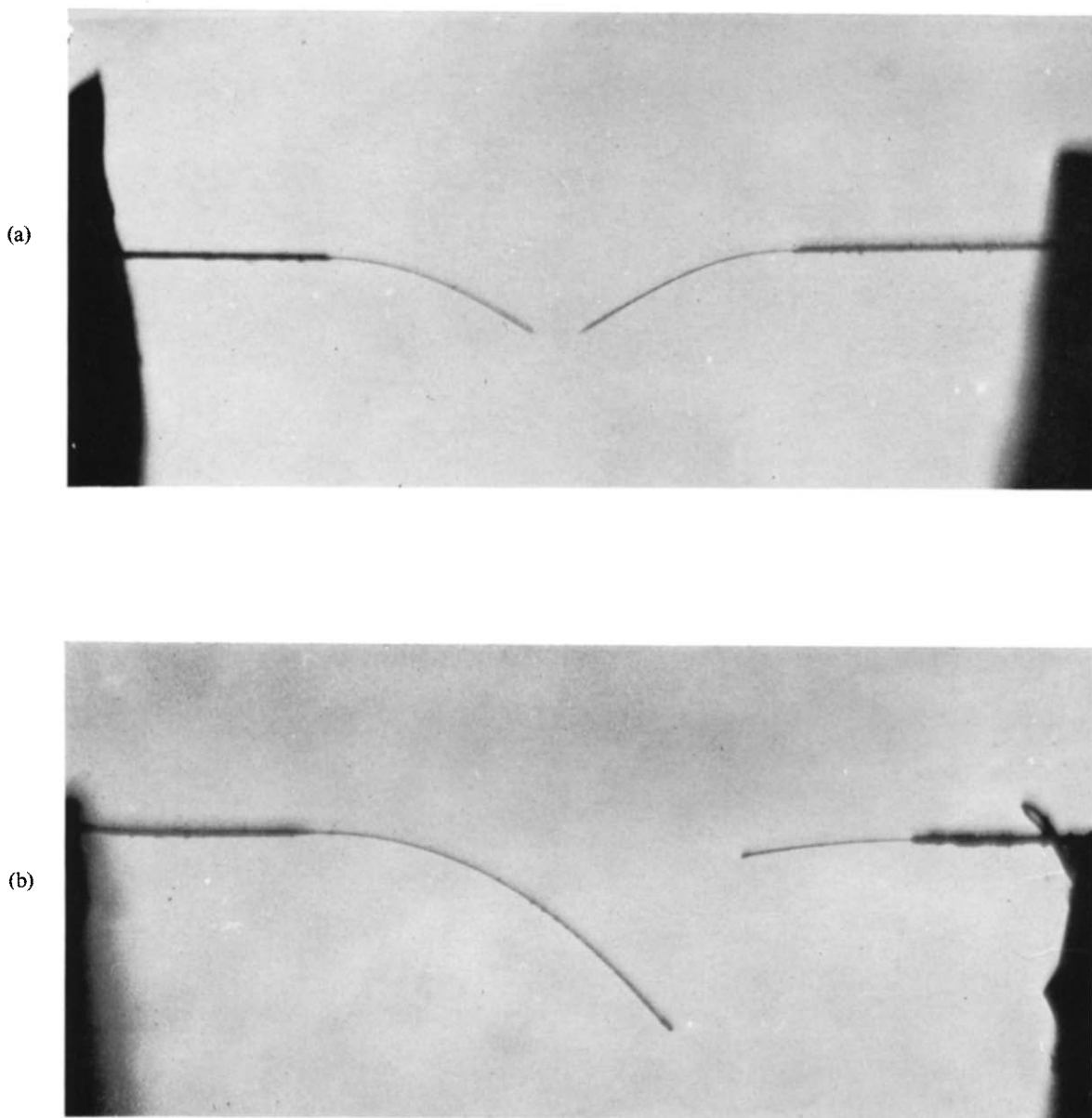


FIG. 11. Location of maximum temperature position on a hot wire by oxidation due to heating.

Wire length = 0.2 cm      Diameter =  $5.1 \times 10^{-4}$  cm

Air flow at atmospheric pressure, speed = 5.2 m/s.

(a) Flow normal to wire      (b) Flow parallel to wire (moving left to right)

of maximum temperature is seen to have moved 25 per cent of the wire length towards the downstream end. Within the accuracy of this experiment, where the wire is heated to more than the normal operating temperature, this result is in agreement with a computed shift of 27 per cent for the same flow conditions (corresponding to Fig. 10a). Champagne [30] measured the distribution of temperature along a wire yawed at  $55^\circ$ , using an infra-red detector to view a 0.001 in. dia. wire. His results indicated a shift of 10 per cent of the wire length for the downstream movement of the peak temperature position at 5.6 m/s, which compares acceptably with an estimate of 8 per cent for this same flow speed by interpolating between the solutions given in Table 2. For the case of flow over a sharply yawed wire the wire length would be the parameter to be used in computing the Péclet number to indicate the extent of cross stream diffusion of heat and thus the different diameter of wire used by Champagne would not be expected to influence the onset of asymmetry generated by this effect.

#### 4. CONCLUSIONS

The application of numerical integration to the iterative solution of the steady energy balance equation for a hot wire has been satisfactorily extended to permit solutions for the surface heat transfer rate over a full range of surface cooling rates in terms of the total measured power loss. The application of this method of calibration to a series of variable density experiments at subsonic Mach numbers has shown that there is an increasing dependence of the surface Nusselt number upon surface temperature as the Knudsen number is reduced. In the limit of large Knudsen numbers ( $> 10$ ) it was found that there was then no dependence of the Nusselt number upon surface temperature. The thermal accommodation coefficient for the tungsten wires used in the air flows was then found to be 0.86. In the limit of small Knudsen numbers, continuum heat-transfer conditions were approached less rapidly at larger values of the

probe Péclet number and larger surface temperatures. The heat loss in conditions approximating to continuum flow was found to depend upon the Péclet number, a behaviour similar to King's law being approached only for large Péclet numbers ( $Pe > 10$ ). The behaviour of cylindrical hot film probes was found to be similar, apart from changes associated with the smaller probe Knudsen numbers.

When a hot wire is yawed to the flow it has been found that the yaw calibration can be approximated by the cosine of the yaw angle raised to some power  $m$ . The index  $m$  was found to vary slightly with the mean yaw angle, particularly at the lower values of the Péclet number. The value obtained for  $m$  was found to reduce with increasing Péclet number, corresponding approximately to the reduction of the index  $n$ .

The development of significant asymmetric heating effects when a probe is yawed to the flow wire has been found to be confined to a range of relatively high yaw angles. The distribution of wire temperature has been calculated in terms of the ratio of the heat loss to the two probe supports. The resulting shift in location of the maximum temperature point has been confirmed by the measurements of Champagne [30] and also by a simple experiment in which the wire was heated to its oxidation temperature. The range of yaw angles over which significant asymmetry was detected was greater at the smaller Péclet numbers. A corollary of the interaction of the thermal wake from upstream sections of the wire on heat transfer from downstream sections is that the overall average Nusselt number calculated from the measured power loss is increased. Such an increase is not unexpected, since the probe is tending towards a slender body rather than a bluff body configuration as the yaw angle becomes large.

In conclusion, it may be seen that the response of cylindrical anemometer probes depends upon a number of distinct convective heat-transfer mechanisms. It has been shown by the results presented that for a range of conditions relevant

to practical anemometry the heat transfer cannot be approximated by any single approximate mathematical model, since there is a significant interaction between the different independent variables. In particular, the interacting effects of Knudsen number, overheat ratio, Péclet number and yaw angle have been demonstrated.

### ACKNOWLEDGEMENTS

The authors gratefully acknowledge the support of the Science Research Council during the course of this investigation, and the availability of facilities at the Universities of Southampton and New South Wales.

### REFERENCES

1. L. V. KING, On the convection of heat from small cylinders in a stream of fluid, *Phil. Trans. R. Soc.* **214A**, 373–432 (1914).
2. P. O. A. L. DAVIES and M. J. FISHER, Heat transfer from electrically heated cylinders, *Proc. R. Soc.* **280A**, 486–527 (1964).
3. J. BOUSSINESQ, An equation for the phenomena of heat convection and an estimate of the cooling power of fluids, *Comptes Rend.* **132**, 1382 (1901). Also, see: *Comptes Rend.* **133**, 257–262 (1901).
4. J. COLE and A. ROSHKO, Heat transfer from wires at Reynolds numbers in the Oseen range, Proceedings, Heat Transfer and Fluid Mechanics Institute, University of California, Berkeley, California (1954).
5. C. R. ILLINGWORTH, Flow at small Reynolds Number, *Laminar Boundary Layers* edited by L. ROSENHEAD. Clarendon Press, Oxford (1963).
6. W. W. WOOD, Calculations for anemometry with fine wires, *J. Fluid Mech.* **32**, 9–20 (1968).
7. C. A. HIEBER and B. GEBHART, Low Reynolds number heat transfer from a circular cylinder, *J. Fluid Mech.* **32**, 21–28 (1968).
8. D. C. COLLIS and M. J. WILLIAMS, Free convection of heat from fine wires, Commonwealth of Australia, Aero. Res. Labs., Aero. Note 140 (1954).
9. D. C. COLLIS and M. J. WILLIAMS, The effects of aspect ratio on convective heat transfer from fine wires, Commonwealth of Australia, Aero. Res. Labs., Aero Note 268 (1966).
10. J. J. MAHONY, Heat transfer at small Grashof numbers, *Proc. R. Soc.* **238A**, 412–423 (1957).
11. W. H. MCADAMS, *Heat Transmission*, 3rd. ed., pp. 252–281. McGraw-Hill, New York (1954).
12. W. J. M. DOUGLAS and S. W. CHURCHILL, Recorrelation of data for convective heat transfer between gases and single cylinders with large temperature differences, *Chem. Engng Prog. Symp. Ser.* **52**, No. 18, 23–28 (1956).
13. L. V. BALDWIN, Slip flow heat transfer from cylinders in subsonic airstreams, N.A.C.A. TN 4369 (1958).
14. L. V. BALDWIN, J. C. LAURENCE and V. A. SANDBORN, Heat transfer from transverse and yawed cylinders in continuum, slip and free molecule flow, *Trans. Am. Soc. Mech. Engrs* **82C**, 77–86 (1960). Also, see: Proceedings, A.S.M.E. Symposium on unsteady flow measurements, Worcester, Mass., (1962).
15. F. M. SAUER and R. M. DRAKE, Forced convection heat transfer from cylinders in a gas, *J. Aero. Sci.* **20**, 175–180 (1953).
16. H. C. LEVY, Heat transfer in low Reynolds number slip flow, *J. Fluid Mech.* **6**, 385–391 (1959).
17. W. WINOVICH and H. A. STINE, Measurements of the non linear variation with temperature of heat transfer rates from hot wires in transonic and supersonic flow, N.A.C.A., TN3965 (1957).
18. W. G. S. SPANGENBERG, Heat loss characteristics of hot wire anemometers at various densities in transonic and supersonic flow, N.A.C.A. TN.3381 (1955).
19. J. H. STALDER, G. GOODWIN and M. O. CREAGER, Heat transfer to bodies in a high speed rarified gas stream, N.A.C.A. Report 1032 (1950).
20. J. H. STALDER, G. GOODWIN and M. O. CREAGER, Heat transfer to bodies in a high speed rarified gas stream, N.A.C.A. Rep. 1093 (1952).
21. A. K. OPPENHEIM, Generalized theory of convective Heat transfer in free molecule flow, *J. Aero. Sci.* **20**, 49–58 (1953).
22. S. BELL and S. A. SCHAAF, Heat transfer to a cylinder for the free molecular flow of a non uniform gas, *Jet Propulsion* **25** (4), 168 et seq. (1955).
23. H. Y. WACHMAN, The thermal accommodation coefficient: A critical survey, *J. Am. Rocket Soc.* **32**, 2–12 (1962).
24. S. A. SCHAAF, Heat transfer in rarified gases, *Developments in Heat Transfer*, chapter 7, pp. 134–168, edited by W. M. ROHSENOW. M.I.T. Press (1964).
25. A. J. MADDEN and E. L. PIRET, Heat transfer from wires to gases at sub-atmospheric pressure under natural convection conditions, I.Mech.E. General Discussion of Heat Transfer, pp. 328–333, London (1951).
26. V. A. SANDBORN and J. C. LAURENCE, Heat loss from yawed hot wires at subsonic Mach numbers, N.A.C.A. TN3563 (1955).
27. C. A. G. WEBSTER, A note on the sensitivity to yaw of the hot wire anemometer, *J. Fluid Mech.* **13**, 307 (1962).
28. J. O. HINZE, *Turbulence*. McGraw-Hill, New York (1959).
29. C. A. FREIHE and W. H. SCHWARZ, Deviations from the cosine law for yawed cylindrical anemometer sensors, *J. Appl. Mech.* **35E**, 655–662 (1968).
30. F. H. CHAMPAGNE, Turbulence measurements with inclined hot wires, Boeing Scientific Research Labs., Document DI-82-0491 (1960).
31. D. C. COLLIS and M. J. WILLIAMS, Two dimensional convection from heated wires at low Reynolds numbers, *J. Fluid Mech.* **6**, (5), 357–384 (1959).
32. J. DELLEUR, Les échanges thermiques de l'anemometre a fils chaud place obliquement dans une ecoulement, *C.R. Acad. Sci., Paris* **259**, 712–714 (1964).

33. H. H. LOWELL, Design and applications of hot wire anemometers for steady state measurements at transonic and supersonic speeds, N.A.C.A., TN 2117 (1950).
34. M. R. DAVIS and P. O. A. L. DAVIES, The physical characteristics of hot wire anemometer. Institute of Sound and Vibration Research, Southampton University, Technical Report 2 (1968).

### FACTEURS INFLUENCANT LE TRANSFERT THERMIQUE A PARTIR DE SONDAS ANEMOMETRIQUES CYLINDRIQUES

**Résumé**—On suppose souvent que les étalonnages de sondes anémométriques à fil ou film chaud dépendent d'une loi entre le nombre de Nusselt relatif à la sonde et le nombre de Reynolds basé sur la composante de vitesse d'écoulement normale à la sonde. En pratique des écarts rencontrés à un tel comportement simplifié sont dus à l'influence de la température de la sonde, aux variations du libre parcours moyen du fluide, aux conditions d'un transfert thermique fini quand la vitesse nulle du fluide est approchée et à l'existence d'effets tridimensionnels dans le refroidissement de sondes en attaque oblique. Dans cet article on discute les effets d'interaction du rapport de surchauffe, du nombre de Knudsen, du nombre de Péclet, du rapport de la longueur au diamètre, du nombre de Grashof et de l'angle d'attaque. En particulier on présente des résultats qui démontrent l'influence du nombre de Péclet et de l'angle d'attaque sur la loi de refroidissement. la variation non linéaire du transfert thermique avec le nombre de Knudsen et les écarts aux réponses symétriques dans des écoulements en attaque oblique. Les mesures rapportées ont été restreintes aux sondes cylindriques à fil et film chauds utilisés à résistance constante.

### FAKTOREN, DIE DEN WÄRMEÜBERGANG AN ZYLINDRISCHEN ANEMOMETERSONDEN BEEINFLUSSEN

**Zusammenfassung**—Es wird oft angenommen, dass die Eichungen von Hitzdraht- und Heissfilm-Anemometersonden von einer Beziehung zwischen der Nusselt-Zahl der Sonde und der mit der zur Sonde senkrechten Geschwindigkeitskomponente gebildeten Reynolds-Zahl abhängen. In Wirklichkeit werden Abweichungen von einem solchen vereinfachten Verhalten festgestellt, die vom Einfluss der Sonden-temperatur, von Änderungen in der mittleren freien Weglänge des Fluids, von den Bedingungen eines endlichen Wärmeübergangs bei verschwindend kleiner Geschwindigkeit und dem Auftreten dreidimensionaler Effekte bei der Kühlung schräggestellter Sonden herrühren. In dieser Arbeit werden die Wechselwirkungen von Überhitzungsverhältnis, Knudsen-Zahl, Peclet-Zahl, Längen-Durchmesser-Verhältnis, Grashof-Zahl und Anstellwinkel erörtert. Insbesondere werden Ergebnisse gebracht, die den Einfluss von Peclet-Zahl und Anstellwinkel auf die Kühlbeziehungen, die Änderung des nichtlinearen Wärmeübergangs mit der Knudsen-Zahl und die Abweichungen bei schräggestellten Sonden von den Ergebnissen bei symmetrischer Anströmung zeigen. Die gezeigten Messungen sind auf zylindrische Hitzdraht- und Heissfilmsonden beschränkt, die bei konstantem Widerstand arbeiten.

### ФАКТОРЫ, ВЛИЯЮЩИЕ НА ПЕРЕНОС ТЕПЛА ОТ ЦИЛИНДРИЧЕСКИХ АНЕМОМЕТРИЧЕСКИХ ЗОНДОВ

**Аннотация**—Обычно считается, что градуировки зондов тепловой проволоки и пленочного анемометра зависят от некоторого соотношения между числом Нуссельта и числом Рейнольдса, определенным по компоненте скорости потока, перпендикулярной к зонду. На практике отклонения от такого упрощенного соотношения встречаются в силу влияния температуры зонда, изменений средней длины свободного пробега молекул среды, условий ограниченного переноса тепла по мере достижения нулевой скорости течения и трехмерных эффектов при охлаждении зондов с наклонными нитями. В статье обсуждаются эффекты взаимодействия степени перегрева, числа Кнудсена и Пекле, отношения длины к диаметру, числа Грасгофа и угла наклона. В частности, представлены результаты, которые демонстрируют влияние числа Пекле и угла наклона на соотношения для охлаждения, изменение нелинейного переноса тепла под влиянием числа Кнудсена и отклонение от симметричных характеристик в потоках, наклонных по отношению к зонду. Представленные результаты измерений ограничены зондами с цилиндрической нагретой нитью и горячей пленкой, действующими при постоянном сопротивлении.